

Non-Markovian Dynamics of Charge Carriers in Quantum Dots

Eduardo Vaz and Jordan Kyriakidis

Department of Physics, Dalhousie University, Halifax, Nova Scotia, Canada, B3H 3J5

E-mail: jordan.kyriakidis@dal.ca

Abstract. We have investigated the dynamics of bound particles in multilevel current-carrying quantum dots. We look specifically in the regime of resonant tunnelling transport, where several channels are available for transport. Through a non-Markovian formalism under the Born approximation, we investigate the real-time evolution of the confined particles including transport-induced decoherence and relaxation. In the case of a coherent superposition between states with different particle number, we find that a Fock-space coherence may be preserved even in the presence of tunneling into and out of the dot. Real-time results are presented for various asymmetries of tunneling rates into different orbitals.

1. Introduction

Some of the most peculiar features of quantum theory, such as the existence of quantum superpositions and of entangled states, are typically destroyed by uncontrolled and ultimately inevitable interactions with a surrounding, often incoherent environment [1].

Most of the recent theoretical analysis done in the area of low-dimensional dynamical quantum systems has been either for open Markovian systems, where the past memory of the system is neglected, or for closed unitary systems, where the dynamics are reversible. Furthermore, much of the research done until recently has focused on steady state phenomena where a Markovian approach can be expected to provide reasonable results.

However, the *transient* behavior of the system carries a tremendous amount of information in the form of coherence and relaxation dynamics. Ultrafast laser pulse excitations, for example, are providing insight into the heterostructure dynamics on a femtosecond timescale [2]. A theory which accounts for quantum dynamical behavior on the same time scale is therefore of great benefit not only to experiment, but also to basic understanding.

The formalism of non-equilibrium Green's functions (NEGF) and formalisms based on NEGF, have been extraordinarily successful in the analysis of much phenomena in mesoscopic systems [3, 4, 5]. Notably, work in both elastic and inelastic transport in quantum dots has been successfully done by means of NEGF or derivatives of this formalism [6, 7]. However, NEGF is inherently a closed-system formalism where the system has Hamiltonian dynamics [8], and thus does not account for irreversibility arising from interactions with an unseen, unknown, or otherwise intractable environment. Promising attempts have been made to extend NEGF to open quantum system, for example, by treating the environment as a correction to the system's self-energy [9], or by calculating two-time correlation functions [10], effectively separating the time scales into transient and steady-state regimes. These and other approaches constitute

significant progress toward a full non-Markovian open system analysis within the NEGF formalism.

Even so, if the evolution of the (possibly correlated) many-body system states themselves are sought, one must calculate the Green's functions and then extract the density matrix, which in the non-equilibrium case may not be unique [10]. An alternative formulation, one we adopt in the sequel, is to work with the density matrix directly. This arguably provides a more intuitive description of the dynamics of non-Markovian open quantum systems, and it readily yields the actual states of the system as well as the quantum coherence between them.

The focus of this paper is to thus present a generic formalism to investigate the dynamics of a few-electron quantum dot in a fully non-Markovian fashion in the density matrix formalism. Section 2 presents a brief outline of the derivation of the evolution equations for the density matrix of the system in both the Markovian and non-Markovian regimes. Section 3 presents the model Hamiltonian for our system as well as the analytical expression for the transition tensor for this model. Section 4 illustrates the non-Markovian approach by considering the case of a multilevel dot in a regime where two channels are available for transport. Results are presented for the transient population probabilities in regimes where the tunnelling strength between system and leads varies from orbital to orbital. In Sec. 5 we give a brief discussion on Fock-space coherences and their implications for Quantum Information. Finally, in Sec. 6, we present a summary and conclusion.

2. Evolution of the density matrix for an open quantum system

In isolated quantum systems, the time evolution can be described by a single state vector $|\psi(t)\rangle$. Once the system is coupled to a larger environment whose degrees of freedom are either unknown, intractable, or uninteresting, the environmental degrees of freedom may be traced out and the resulting state of the system alone is described not by a state vector, but by a density operator [11] $\rho(t) = \sum_n W_n(t) |\psi_n(t)\rangle \langle \psi_n(t)|$, where $W_n(t)$ is the probability that state $|\psi_n(t)\rangle$ is occupied at time t . The time-dependence of the density operator can be obtained by an iterative integration of the Liouville-von Neumann equation, which gives

$$\dot{\rho}(t) = -\mathcal{L}(t)\rho(0) + \int_0^t dt' \mathcal{L}(t)\mathcal{L}(t')\rho(t') + \int_0^t dt' \int_0^{t'} dt'' \mathcal{L}(t)\mathcal{L}(t')\mathcal{L}(t'')\rho(t'') + \dots, \quad (1)$$

where $\mathcal{L}(t)$ is a Liouville superoperator such that, $\mathcal{L}(t)F = i\hbar^{-1}[H(t), F]$ for any operator F and Hamiltonian $H(t)$.

Equation (1) represents the evolution of the complete system plus environment. Under the Born approximation, the evolution equations are truncated at second order in the interaction Hamiltonian. After some manipulation [11], the resulting equations for the matrix elements of the density operator read,

$$\dot{\rho}_{ab}(t) = \sum_{c,d} \int_0^t dt' \rho_{cd}(t') R_{abcd}(t-t') e^{i\gamma_{abcd}t'}, \quad (2)$$

where, $R_{abcd}(t-t')$ is a Redfield-type transition tensor containing all the information characterizing the system, the environment, and the coupling between them, and where $\gamma_{abcd} = \omega_{ab} - \omega_{cd} = (E_a - E_b + E_d - E_c)/\hbar$ denotes energy differences between system states.

For an environment with a much greater number of degrees of freedom relative to those of the system, and for a weak enough system-environment coupling, we make the assumption that the system has no effect (no back-action) on the environment, that the system is not correlated with the environment, and that the environment is and remains in equilibrium [11]. In this case, the total density matrix for the system plus environment can be written as,

$$\rho(t) \approx \rho_{\text{system}}(t) \rho_{\text{R}}(0). \quad (3)$$

where $\rho_{\text{system}}(t)$ is the density matrix for the open quantum system, and ρ_{R} is the density matrix for the environment.

2.1. Markovian Approach

The Markov approximation assumes an environment which relaxes on a time scale time much faster than the characteristic time of the system. The environment correlation functions vanish at such a fast rate, that the reversibility of the system is essentially destroyed, thus also destroying the memory of the system [1]. Thus, $\dot{\rho}_{\text{system}}(t)$ depends only on the present value of $\rho(t)$. That is, it becomes local in time. For time intervals $t-t'$ much greater than the environment's correlation time τ , the correlation functions for environment operators rapidly become uncorrelated and decay to zero, $\langle F_k^\dagger(t-t')F_{k'} \rangle \approx \langle F_k^\dagger(t-t') \rangle \langle F_{k'} \rangle \approx 0$. In the limit $t-t' \gg \tau$ the upper integration limit in (2) can be extended to infinity with negligible error in the calculations. Since the time when the coupling is turned on is arbitrary, the lower integration limit can be taken to negative infinity, and the coupled set of integro-differential evolution equations become a coupled set of first order ordinary differential equations:

$$\dot{\rho}_{ab}(t) \longrightarrow \sum_{cd} \rho_{cd}(t) \int_{-\infty}^{\infty} dt' R_{abcd}(t-t') e^{i\gamma_{abcd}t'} = \sum_{cd} \rho_{cd}(t) W_{abcd}. \quad (4)$$

This in turn leads to a Fermi's Golden rule for transitions with strict energy conservation for all transitions.

Although much of the recent theory in the area of non-equilibrium quantum dot systems has made use of Markovian-type approximations [12, 13, 14, 15, 16, 17], the approach has fairly severe consequences on the transient behavior of the system, especially when considering coherence properties of the system at short time scales. Nonetheless, the Markov approximation may be expected to yield reasonable results at sufficiently long times [11], when the system has reached a steady state, or when considering intermediate time scales of averaged behavior, such as the average total current through a system.

2.2. Non-Markovian Approach

In order to account for the transient dynamics, especially for the characteristics of the coherence between system states, memory effects must be preserved. In our approach we make use of the convolution theorem for Laplace transforms, to represent Eq. (2) as a set of algebraic equations in Laplace space,

$$s\rho_{ab}(s + i\omega_{ab}) - \rho(0) = \sum_{cd} \rho_{cd}(s + i\omega_{cd}) R_{abcd}(s + i\omega_{ab}). \quad (5)$$

This set of coupled algebraic equations can be solved analytically for $\rho_{ab}(s)$ for only a few system states ($\sim 2-4$), since the computational effort rapidly increases with the number of available transport channels. In the regime of sequential resonant tunnelling transport through a quantum dot containing non-interacting electrons, the transport channels are those single-particle system states $|\alpha\rangle$, whose energy lies within the bias window. These single-particle states define the possible dynamical many-body states of the system as those involved when the single particle states are empty or occupied. Thus, for k channels, a minimum of 2^k many-body system states are required (for empty or occupied). Furthermore, $(2^k)^2$ density-matrix elements are required to describe the population probabilities as well as the coherence between the states. The temporal evolution of the density-matrix elements themselves are governed by $(2^k)^4$ transition tensor elements (Redfield-type in the Born approximation). For larger sizes, a numerical approach may be utilised to invert the linear system in Eq. (5) at each (complex-valued) point s , thus obtaining $\rho_{ab}(s)$. The solutions $\rho_{ab}(s)$ in Laplace space can then be

brought back to time space by applying an inverse Laplace transform. This is done numerically by performing a Bromwich integral [18] over a suitably chosen contour. For every point s along the Bromwich contour, a matrix inversion is performed to evaluate all components of $\rho_{ab}(s)$. Such a Bromwich integration is (numerically) performed [19] at each time step, thus obtaining $\rho_{ab}(t)$.

2.3. Violation of Positivity

It has been established by Kraus [20], Lindblad [21], and Gorini, Kossakowki, and Sudarshan [22], that the evolution of an open quantum system must remain completely positive to ensure the physical validity of the states of the system at all times. However, this positivity may be broken by introduction of ad hoc relaxation rates, by the choice of basis states, or by the truncation of higher-order interaction terms in the evolution equations (such as in the Born approximation), which can yield serious inconsistencies such as negative probabilities. Despite this, much of the investigations of non-Markovian dynamics acknowledge that for a set of initial conditions, the theory will reproduce physically consistent results. Our findings agree with this premise [23].

3. Model

We model our system as a single generic quantum dot coupled to a source and a drain reservoir by a tunneling Hamiltonian [24]. The total Hamiltonian is given by,

$$H = H_S + H_{QD} + H_D + H_T, \quad (6a)$$

where H_S and H_D are the source and drain Hamiltonians, respectively. These are taken to be non-interacting Fermion systems shifted by the bias:

$$H_{S(D)} = \sum_{s(d)} (\epsilon_{s(d)} \pm \frac{1}{2} eV_B) d_{s(d)}^\dagger d_{s(d)}, \quad (6b)$$

with $d_{s(d)}^\dagger$ a creation operator for the source (drain), and $d_{s(d)}$ an annihilation operator.

The Hamiltonian for the quantum dot in Eq.(6a) is given by,

$$H_{QD} = \sum_i (\hbar\omega_i + eV_g) c_i^\dagger c_i + V_{\text{int}}, \quad (6c)$$

where the single-particle energies $\hbar\omega_i$ are all shifted by the applied gate voltage, and V_{int} is the interaction among the confined particles.

The tunneling Hamiltonian describing the reservoir-dot coupling is given by,

$$H_T = \sum_{k,r=(s,d)} \left(T_k^r d_r^\dagger c_k + h.c \right), \quad (6d)$$

where $T_k^{s(d)}$ is an energy-independent tunneling coefficient for a particle tunneling from the single-particle state $|k\rangle$ in the dot to the source (drain) reservoir. Finally, we assume zero temperature such that the reservoirs are in their respective non-degenerate ground states.

As mentioned above, all system and environment information, including the characteristics of the interaction between them are contained in the memory kernel, $R_{abcd}(\tau)$ appearing in Eq.(2). For the model in Eq. (6), we obtain

$$R_{abcd}(\tau) = \sum_{\alpha,\beta,R} K_{\alpha\beta}^R(\tau) \left\{ \Omega_{\phi_B,\mu^R}^\alpha \Delta_{badc}^{\alpha\beta} - \Omega_{\phi_T,\mu^R}^\alpha \Delta_{cdab}^{\alpha\beta} \right\} \\ + K_{\beta\alpha}^R(\tau) \left\{ (\Omega_{\phi_B,\mu^R}^\alpha)^* \Delta_{abcd}^{\alpha\beta} - (\Omega_{\phi_T,\mu^R}^\alpha)^* \Delta_{dcba}^{\alpha\beta} \right\}, \quad (7)$$

where the indices a , b , c , and d denote many-body states, α , and β are denote single-particle states, and $R = S, D$ runs over the source and drain leads. The energy $\phi_{T(B)}$ denotes the top (bottom) of the band, and μ^R is the chemical potential of reservoir R . Furthermore, we have defined

$$\Omega_{x,y}^\alpha \equiv e^{i\omega_{x,\alpha}\tau} - e^{i\omega_{y,\alpha}\tau}, \quad (8a)$$

$$\Delta_{abcd}^{\alpha,\beta} \equiv \langle a|c_\alpha^\dagger|c\rangle\langle d|c_\beta|b\rangle - \langle a|c\rangle\langle b|c_\alpha c_\beta^\dagger|d\rangle, \quad (8b)$$

and

$$K_{\alpha,\beta}^R(\tau) \equiv \frac{iN_R}{\hbar\tau} (T_\alpha^* T_\beta)_R, \quad (8c)$$

where $\omega_{x,\alpha} = (E_x - E_\alpha)/\hbar$ is a frequency denoting the energy difference between states $|x\rangle$ and $|\alpha\rangle$, T_α is the tunneling coefficient to a single particle state $|\alpha\rangle$ in the dot, N_R is the density of states for the 2DEG environment, and τ is a time parameter.

With this general form for the transition tensor, given a set of basis states, the individual elements of the tensor are calculated. The form of the Redfield transition tensor allows for independent tuning and analysis of barrier width symmetries, and of asymmetries between core-states and edge-states couplings to the reservoirs, by means of the independent tunneling rates.

4. Two-channel (four-state) system

As an illustrative example, we present results for the diagonal elements of $\rho(t)$ in the above model. For definiteness, we consider a quantum dot with N confined particles, and with two resonant tunnelling transport channels available within the bias window. Each channel involves a particle-number fluctuation between N and $N \pm 1$, and can involve either the ground or first excited state of the N -particle system. In general, the availability of k transport channels involves a minimum of 2^k states. In the present case, the four relevant states are

$$|0\rangle = |(N-1)_{g.s.}\rangle, \quad |1\rangle = |N_{g.s.}\rangle, \quad |2\rangle = |(N+1)_{g.s.}\rangle, \quad |3\rangle = |(N)_{e.s.}\rangle. \quad (9)$$

Here, the state $|0\rangle$ denotes the $(N-1)$ -particle ground state of the system, $|1\rangle$ and $|2\rangle$ denote ground-states of the N and $(N+1)$ -particle system respectively, and $|3\rangle$ denotes the first excited state of the N -particle system. A schematic representation of the system is shown in Fig. 1.

Each orbital will in general be coupled differently to the leads, owing to the detailed shape of the wave function [25]. We identify in Fig. 1 edge and core orbitals. Core orbitals are weakly coupled to the leads owing to a poor (s -type) overlap with the lead states whereas edge orbitals (p -type) are more strongly coupled to the leads.

Figure 2 shows the real-time evolution of the population probabilities of the system $\rho_{nn}(t)$ in the large bandwidth limit. Results are shown for a bias of $V_{\text{bias}} = 6$ meV, symmetric about the Fermi energy ϵ_{Fermi} . We assume two channels within the bias window, $E_\alpha = \epsilon_{\text{Fermi}} + 1$ meV and $E_\beta = \epsilon_{\text{Fermi}} - 1$ meV. Finally, we keep the barriers fully symmetric (i.e. $T^{\text{source}} = T^{\text{drain}}$), while the ratio between tunneling to core states and tunneling to edge states, is varied (i.e. $T^\alpha/T^\beta > 1$). Several features are evident in Fig. 2, and we discuss three in particular.

First, we see that for the smallest couplings to the core orbitals (the two plots on the right of Fig. 2), the four levels couple into two distinct pairs. States $|1\rangle$ and $|2\rangle$ —the N and $(N+1)$ -particle ground states—are strongly coupled, as are states $|0\rangle$ and $|3\rangle$ —the $(N-1)$ -particle ground state and the N -particle first-excited state. We can understand why this occurs with recourse to Fig. 1. The transition between states $|1\rangle$ and $|2\rangle$ is through an edge orbital and this coupling is stronger than the transition between $|1\rangle$ and $|0\rangle$ which involves a core orbital. Similar

arguments apply for the coupling between states $|3\rangle$ and $|0\rangle$ (strong coupling) and between $|3\rangle$ and $|2\rangle$ (weak coupling).

Second, in the steady state ($t \rightarrow \infty$), all occupation probabilities tend to the same value of $1/4$. This is seen regardless of the tunnelling strengths of core and edge states. The equal probability of $1/4$ for each level can be understood as being due to the symmetric barriers between the dot and the source on the one hand, and between the dot and the drain on the other. Since these barriers are symmetric, any level will have an equal probability of being either occupied or unoccupied.

Third, although all four states are equally occupied in the steady state, the time to *actually reach* the steady states does depend on the relative couplings to the core and edge orbitals. The fact that the time taken to reach the steady state increases as the tunnelling to the core state decreases can be understood as the effect of decreasing the available tunnelling pathways. Fewer pathways available means that the system takes longer to reach the steady state. In the limit of zero tunnelling to the core state, for example, states $|3\rangle$ and $|0\rangle$ will *never* become occupied. In this case, the remaining two levels will each reach an occupation probability of $1/2$ rather than $1/4$.

5. Fock-Space Coherence

Finally, we comment on the various forms of coherence available to systems like the present one in which the particle number fluctuates. By Hilbert-space coherence, we denote coherence between states with identical particle numbers—states $|1\rangle$ and $|3\rangle$ in Eq. (9), for example. In contrast, a Fock-space coherence can exist between states of differing particle number. In the system considered above, we can have a Fock-space coherence between states differing by one particle—four possibilities for the states in Eq. (9)—or by two particles—states $|0\rangle$ and $|2\rangle$. In general, the interaction and interplay between these distinct classes of coherence is governed by the Redfield tensor $R_{abcd}(t)$.

For the $k = 2$ channel system, $k^2 = 4$ four states are required, as outlined above. This yields $(k^2)^2 = 16$ density matrix elements, and thus, $(k^2)^4 = 256$ Redfield tensor components, many of which are not independent and many of which vanish. In Fig. 3 we show a graphical representation of all non-zero components of the Redfield tensor, for the same 2-channel case described above for the model Eq. (6). In this matrix representation, we see three distinct and decoupled submatrices. The top submatrix represents the transitions between the population probabilities and all Hilbert-space coherence terms. The remaining two block describe the

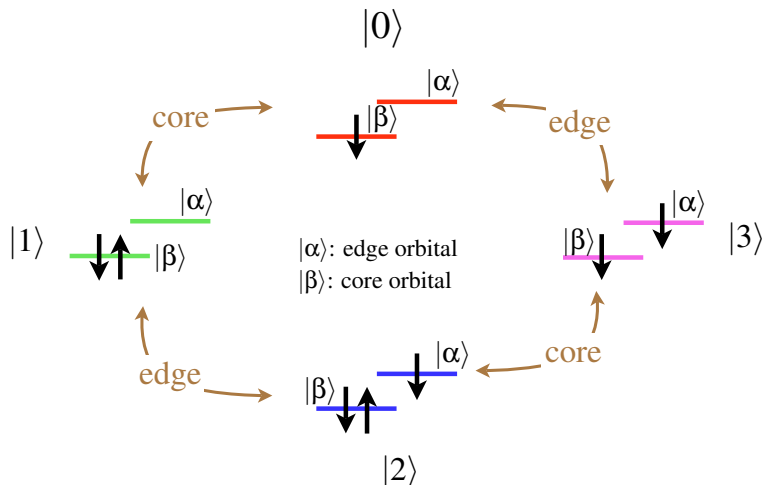


Figure 1. Schematic representations of system under consideration. Four system states are considered depending on the relative occupation of the single-particle orbitals $|\alpha\rangle$ and $|\beta\rangle$, each of which can in principle have different tunnel couplings to the leads.

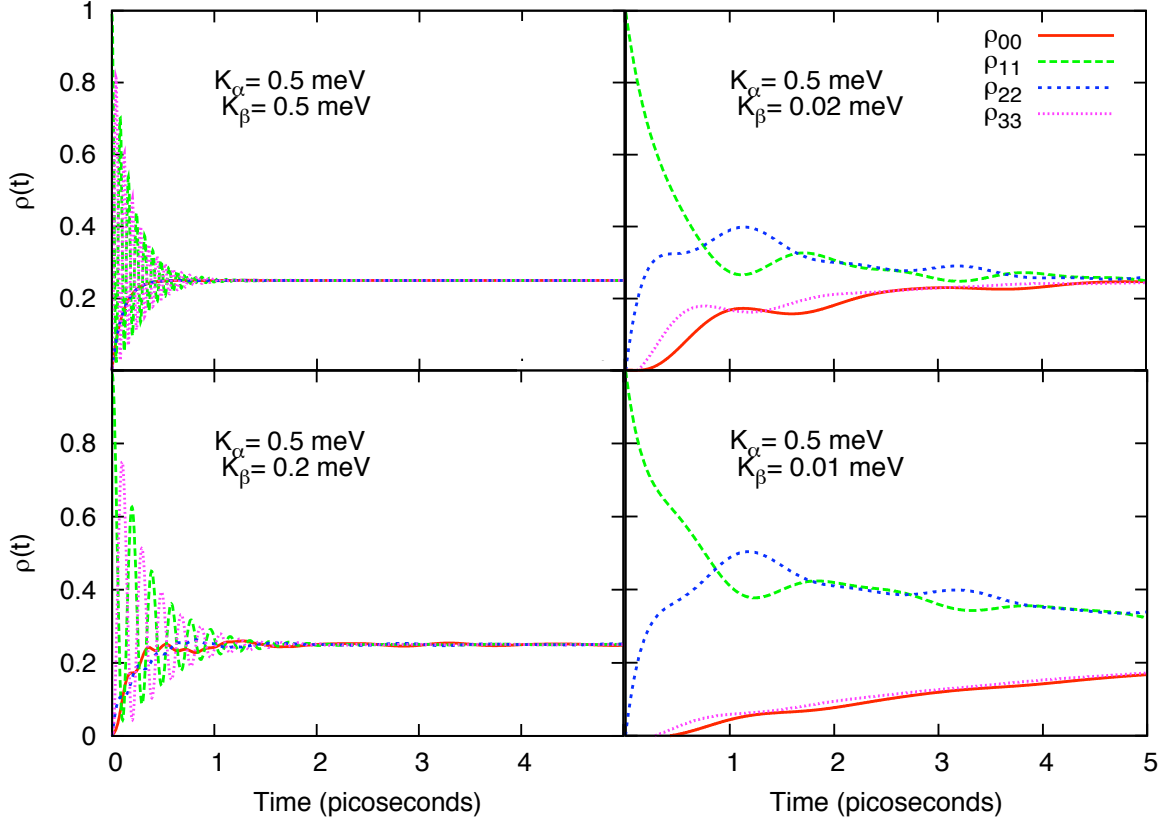


Figure 2. Time evolution of population probabilities in a quantum dot with 2 transport channels and four states. (See Eq. (9).) The plots are for symmetric source and drain tunnel barriers, and varying core edge asymmetry. We assume a 6 meV bias symmetric about the Fermi energy, and two transport channels at energies $\epsilon_{\text{Fermi}} \pm 1$ meV.

Fock-space coherence between states differing by either one (middle submatrix) or two (bottom submatrix) particles.

The remarkable structure evident in Fig. 3 implies that each block undergoes its own independent time evolution. In turn, this suggests that, should a Fock-space coherence be established in the system at any time, this coherence can be robust and long-lived even in the rather severe perturbation of transport carriers being continually injected and removed from the system. This may have very promising consequences for quantum information, where strong, accessible, and long-lived coherence is an essential prerequisite for information processing beyond the classical limit.

6. Conclusion

We have developed a generic non-Markovian formalism for the real-time evolution of the density matrix of a quantum dot weakly coupled to source and drain reservoirs. Within the tunneling Hamiltonian approach, we have analytically derived an explicit transition (Redfield) tensor describing the full dynamics of the system. In the case of two transport channels (four states) we observed the real-time evolution of the population probabilities, taking account differing tunnelling rates to different orbitals. Two distinct types of coherence became evident from the results, a Hilbert space coherence between states with same particle number, and a Fock-space coherence between states with different particle numbers. Under appropriate conditions,

	ρ_{00}	ρ_{11}	ρ_{22}	ρ_{33}	ρ_{13}	ρ_{31}	ρ_{01}	ρ_{10}	ρ_{03}	ρ_{30}	ρ_{12}	ρ_{21}	ρ_{32}	ρ_{23}	ρ_{02}	ρ_{20}
ρ_{00}	R ₀₀₀₀	R ₀₀₁₁	0	R ₀₀₃₃	R ₀₀₁₃	R ₀₀₃₁	0	0	0	0	0	0	0	0	0	0
ρ_{11}	R ₁₁₀₀	R ₁₁₁₁	R ₁₁₂₂	0	R ₁₁₁₃	R ₁₁₃₁	0	0	0	0	0	0	0	0	0	0
ρ_{22}	0	R ₂₂₁₁	R ₂₂₂₂	R ₂₂₃₃	R ₂₂₁₃	R ₂₂₃₁	0	0	0	0	0	0	0	0	0	0
ρ_{33}	R ₃₃₀₀	0	R ₃₃₂₂	R ₃₃₃₃	R ₃₃₁₃	R ₃₃₃₁	0	0	0	0	0	0	0	0	0	0
ρ_{13}	R ₁₃₀₀	R ₁₃₁₁	R ₁₃₂₂	R ₁₃₃₃	R ₁₃₁₃	0	0	0	0	0	0	0	0	0	0	0
ρ_{31}	R ₃₁₀₀	R ₃₁₁₁	R ₃₁₂₂	R ₃₁₃₃	0	R ₃₁₃₁	0	0	0	0	0	0	0	0	0	0
ρ_{01}	0	0	0	0	0	0	R ₀₁₀₁	0	R ₀₁₀₃	0	R ₀₁₁₂	0	R ₀₁₂₃	0	0	0
ρ_{10}	0	0	0	0	0	0	0	R ₁₀₁₀	0	R ₁₀₃₀	0	R ₁₀₂₁	0	R ₁₀₂₃	0	0
ρ_{03}	0	0	0	0	0	0	R ₀₃₀₁	0	R ₀₃₀₃	0	R ₀₃₁₂	0	R ₀₃₃₂	0	0	0
ρ_{30}	0	0	0	0	0	0	0	R ₃₀₁₀	0	R ₃₀₃₀	0	R ₃₀₂₁	0	R ₃₀₂₃	0	0
ρ_{12}	0	0	0	0	0	0	R ₁₂₀₁	0	R ₁₂₀₃	0	R ₁₂₁₂	0	R ₁₂₃₂	0	0	0
ρ_{21}	0	0	0	0	0	0	0	R ₂₁₁₀	0	R ₂₁₃₀	0	R ₂₁₂₁	0	R ₂₁₂₃	0	0
ρ_{32}	0	0	0	0	0	0	R ₃₂₀₁	0	R ₃₂₀₃	0	R ₃₂₁₂	0	R ₃₂₃₂	0	0	0
ρ_{23}	0	0	0	0	0	0	0	R ₂₃₁₀	0	R ₂₃₃₀	0	R ₂₃₂₁	0	R ₂₃₂₃	0	0
ρ_{02}	0	0	0	0	0	0	0	0	0	0	0	0	0	0	R ₀₂₀₂	0
ρ_{20}	0	0	0	0	0	0	0	0	0	0	0	0	0	0	0	R ₂₀₂₀

Figure 3. Representation of the non-zero Redfield tensor elements for the non-interacting, non-Markovian theory for the 2 transport-channel case with the four-states: $|0\rangle = |(N-1)_{g.s.}\rangle$, $|1\rangle = |N_{g.s.}\rangle$, $|2\rangle = |(N+1)_{g.s.}\rangle$, and $|3\rangle = |(N)_{e.s.}\rangle$. Three distinct decoupled submatrices become apparent: The top submatrix represents the transitions between the population probabilities and the coupled coherence between them (Hilbert-space coherence), the middle submatrix represents transitions relating states with particle numbers differing by 1, and the bottom submatrix (a 1 by 1 matrix) represents a transition relating states with particle numbers differing by 2.

the Fock-space coherence is decoupled from the evolution of the rest of the system, suggesting promising consequences for quantum information processing.

Acknowledgments

This work is supported by the Natural Sciences and Engineering Research Council of Canada, by the Canadian Foundation for Innovation, and by Dalhousie University. The authors acknowledge illuminating discussions with Jean-Marc Samson and Catherine Stevenson.

References

- [1] Breuer H P and Petruccione F 2002 *The theory of open quantum systems* (New York: Oxford University Press)
- [2] Shah J 1999 *Ultrafast Spectroscopy of Semiconductors and Semiconductor Nanostructures* (New York: Springer)
- [3] Kadanoff L P and Baym G 1962 *Quantum Statistical Mechanics* (New York: W. A. Benjamin Inc)
- [4] Haug H and Koch S 1990 *Quantum Theory of the Optical and Electronic Properties of Semiconductors* (Singapore: World Scientific)

- [5] Haug H and Jauho A P 1996 *Quantum Kinetics in Transport and Optics of Semiconductors* (Berlin: Springer)
- [6] Wacker A and Jauho A P 1998 *Phys. Rev. Lett.* **80** 369–372
- [7] Wacker A, Jauho A P, Rott S, Markus A, Binder P and Döhler G H 1999 *Phys. Rev. Lett.* **83** 836–839
- [8] Datta S 1995 *Electronic Transport in Mesoscopic Systems* (Cambridge: Cambridge University Press)
- [9] Datta S 2000 *Superlattice. Microst.* **28** 253–278
- [10] Knezevic I and Ferry D 2003 *Phys. Rev. E* **67** 066122
- [11] Blum K 1996 *Density Matrix Theory and Applications* (New York: Springer)
- [12] Apalkov V M 2007 *Phys. Rev. B* **75** 5
- [13] Imura K, Utsumi Y and Martin T 2007 *Physical Review B* **75** 205341
- [14] Pedersen J N, Lassen B, Wacker A and Hettler M H 2007 *Phys. Rev. B* **75** 235314
- [15] Egorova D, Thoss M, Domcke W and Wang H 2003 *J. Chem. Phys.* **119** 2761
- [16] Legel S, König J, Burkard G and Schön G 2007 *Phys. Rev. B* **76** 085335
- [17] Vaz E and Kyriakidis J 2006 *Arxiv preprint: cond-mat/0608272*
- [18] Abramowitz M and Stegun I A 1964 *Handbook of Mathematical Functions with Formulas, Graphs, and Mathematical Tables* (New York: Dover)
- [19] The Bromwich integral is evaluated using an adaptive Fourier integration routine using tables of Chebyshev moments. See, for example, the QAWF algorithms in the GNU scientific library (<http://www.gnu.org/software/gsl>).
- [20] Kraus K 1971 *Ann. Phys. (N. Y.)* **64** 311
- [21] Lindblad G 1976 *Commun. Math. Phys.* **48** 119
- [22] Gorini V, Kossakowski A and Sudarshan E 1976 *J. Math. Phys.* **17** 821
- [23] Vaz E and Kyriakidis J Unpublished
- [24] Mahan G D 1981 *Many-particle Physics* (New York: Plenum)
- [25] Ciorga M, Wensauer A, Pioro-Ladriere M, Korkusinski M, Kyriakidis J, Sachrajda A S and Hawrylak P 2002 *Phys. Rev. Lett.* **88** 256804